



Protein Phosphatase 1 Inhibitor-1 Mediates the cAMP-Dependent Stimulation of the Renal NaCl Cotransporter

Penton, David ; Moser, Sandra ; Wengi, Agnieszka ; Czogalla, Jan ; Rosenbaek, Lena Lindtoft ; Rigendinger, Fritz ; Faresse, Nouridine ; Martins, Joana R ; Fenton, Robert A ; Loffing-Cueni, Dominique ; Loffing, Johannes

Abstract: Background: A number of cAMP-elevating hormones stimulate phosphorylation (and hence activity) of the NaCl cotransporter (NCC) in the distal convoluted tubule (DCT). Evidence suggests that protein phosphatase 1 (PP1) and other protein phosphatases modulate NCC phosphorylation, but little is known about PP1's role and the mechanism regulating its function in the DCT. Methods: We used ex vivo mouse kidney preparations to test whether a DCT-enriched inhibitor of PP1, protein phosphatase 1 inhibitor-1 (I1), mediates cAMP's effects on NCC, and conducted yeast two-hybrid and coimmunoprecipitation experiments in NCC-expressing MDCK cells to explore protein interactions. Results: Treating isolated DCTs with forskolin and IBMX increased NCC phosphorylation via a protein kinase A (PKA)-dependent pathway. Ex vivo incubation of mouse kidney slices with isoproterenol, norepinephrine, and parathyroid hormone similarly increased NCC phosphorylation. The cAMP-induced stimulation of NCC phosphorylation strongly correlated with the phosphorylation of I1 at its PKA consensus phosphorylation site (a threonine residue in position 35). We also found an interaction between NCC and the I1-target PP1. Moreover, PP1 dephosphorylated NCC in vitro, and the PP1 inhibitor calyculin A increased NCC phosphorylation. Studies in kidney slices and isolated perfused kidneys of control and I1-KO mice demonstrated that I1 participates in the cAMP-induced stimulation of NCC. Conclusions: Our data suggest a complete signal transduction pathway by which cAMP increases NCC phosphorylation via a PKA-dependent phosphorylation of I1 and subsequent inhibition of PP1. This pathway might be relevant for the physiologic regulation of renal sodium handling by cAMP-elevating hormones, and may contribute to salt-sensitive hypertension in patients with endocrine disorders or sympathetic hyperactivity.

DOI: <https://doi.org/10.1681/asn.2018050540>

Posted at the Zurich Open Repository and Archive, University of Zurich

ZORA URL: <https://doi.org/10.5167/uzh-170339>

Journal Article

Accepted Version

Originally published at:

Penton, David; Moser, Sandra; Wengi, Agnieszka; Czogalla, Jan; Rosenbaek, Lena Lindtoft; Rigendinger, Fritz; Faresse, Nouridine; Martins, Joana R; Fenton, Robert A; Loffing-Cueni, Dominique; Loffing, Johannes (2019). Protein Phosphatase 1 Inhibitor-1 Mediates the cAMP-Dependent Stimulation of the Renal NaCl Cotransporter. *Journal of the American Society of Nephrology (JASN)*, 30(5):737-750.

DOI: <https://doi.org/10.1681/asn.2018050540>

Author's Copy

Protein phosphatase 1 inhibitor 1 mediates the cAMP-dependent stimulation of the renal NaCl cotransporter

David Penton^{1,2}, Sandra Moser¹, Agnieszka Wengi¹, Jan Czogalla^{1,2}, Lena Lindtoft Rosenbaek^{3,4}, Fritz Rigendinger¹, Nourdine Faresse^{1,2}, Joana R. Martins^{1,2}, Robert A. Fenton³, Dominique Loffing-Cueni¹, Johannes Loffing^{1,2}

¹Institute of Anatomy, University of Zurich, Switzerland; ²Swiss National Centre for Competence in Research "Kidney control of homeostasis"; ³Department of Biomedicine, Aarhus University, Denmark; Department of Neuroscience, University of Copenhagen

Article Information

ASN.2018050540

DOI

<https://doi.org/10.1681/ASN.2018050540>

PubMed

[30902838](#)

Published By

[American Society of Nephrology](#)

Print ISSN

[1046-6673](#)

I1 mediates cAMP stimulation of NCC

Online ISSN

[1533-3450](#)

History

- Received for publication May 22, 2018
- Accepted for publication February 6, 2019
- Published online March 22, 2019.

Online version:

<https://jasn.asnjournals.org/content/early/2019/03/22/ASN.2018050540>

Protein phosphatase 1 inhibitor 1 mediates the cAMP-dependent stimulation of the renal NaCl cotransporter

David Penton^{1,2}, Sandra Moser¹, Agnieszka Wengi¹, Jan Czogalla^{1,2}, Lena Lindtoft Rosenbaek^{3,4}, Fritz Rigendinger¹, Nourdine Faresse^{1,2}, Joana R. Martins^{1,2}, Robert A. Fenton³, Dominique Loffing-Cueni¹, Johannes Loffing^{1,2}

¹Institute of Anatomy, University of Zurich, Switzerland; ²Swiss National Centre for Competence in Research "Kidney control of homeostasis"; ³Department of Biomedicine, Aarhus University, Denmark; Department of Neuroscience, University of Copenhagen

Running title:

I1 mediates cAMP stimulation of NCC

Corresponding author:

Johannes Loffing

University of Zurich, Institute of Anatomy

Winterthurerstrasse 190, CH-8057 Zurich

Switzerland

Phone: +41 (0) 44 635 53 20

Fax: + 41 (0) 44 635 57 02

Email: johannes.loffing@anatom.uzh.ch

Significance statement:

The thiazide-sensitive NaCl cotransporter (NCC) in the distal convoluted tubule (DCT) is critical for the renal control of ion homeostasis and blood pressure. NCC phosphorylation, and hence activity, is increased by cAMP-elevating stimuli, including β -adrenergic agonists and PTH. We tested the hypothesis that the inhibitor 1 (I1) of protein phosphatase 1 (PP1) mediates the effects of cAMP-elevating hormones on NCC. Using several *in vitro* and *ex vivo* approaches, we propose a novel signaling pathway in which a PKA-dependent phosphorylation of I1 inhibits the PP1-dependent dephosphorylation of NCC. This novel pathway may contribute to the physiological regulation of NCC and the development of arterial hypertension in the context of abnormal hormonal stimulation.

Abstract

Background: The NaCl cotransporter (NCC) in the distal convoluted tubule (DCT) is critical for renal Na⁺ reabsorption and blood pressure control. A number of cAMP-elevating hormones stimulate NCC phosphorylation, and hence activity.

Methods: Using a variety of experiments on mouse *ex vivo* kidney preparations, we tested the hypothesis that the DCT-enriched protein phosphatase 1 inhibitor 1 (I1) mediates the effects of cAMP on NCC.

Results: Treatment of isolated DCTs with forskolin and IBMX increased the phosphorylation of NCC via a protein kinase A (PKA)-dependent pathway. Likewise, *ex vivo* incubation of mouse kidney slices with isoproterenol, norepinephrine and PTH increased NCC phosphorylation. The cAMP-induced stimulation of NCC phosphorylation strongly correlated with the phosphorylation of I1 at its PKA consensus site (T35). Yeast two-hybrid and co-immunoprecipitation experiments in NCC-expressing MDCK cells indicated an interaction between NCC and the I1-target PP1. Moreover, PP1 dephosphorylated NCC *in vitro* and the PP1 inhibitor calyculin A increased NCC phosphorylation. Studies on kidney slices and isolated perfused kidneys of control and I1-KO mice demonstrated that I1 participates to the cAMP-induced stimulation of NCC.

Conclusion: Our data suggests a complete signal transduction pathway by which cAMP increases NCC phosphorylation via a PKA-dependent phosphorylation of I1 and subsequent inhibition of PP1. This pathway might be relevant for the physiological regulation of renal Na⁺ handling by cAMP-elevating hormones and may contribute to salt-sensitive hypertension in patients with endocrine disorders or sympathetic hyperactivity.

Keywords:

NaCl cotransporter, β -adrenergic stimulation, PKA, protein phosphatase 1, protein phosphatase 1 inhibitor 1

Introduction

The thiazide-sensitive NaCl cotransporter (NCC) in the renal distal convoluted tubule (DCT) is crucial for the fine-tuning of renal sodium (Na^+) reabsorption and hence for the control of blood pressure. NCC and the DCT are also critically involved in the renal control of potassium (K^+), magnesium (Mg^{2+}), calcium (Ca^{2+}) and acid/base homeostasis¹. The crucial role of NCC is evidenced by genetic diseases in which loss of function mutations of NCC cause Gitelman syndrome featuring hypokalemic alkalosis, hypomagnesemia, hypocalciuria and lowered arterial blood pressure². Conversely, enhanced NCC activity due to mutations in its regulating kinases, namely the **with no lysine (K)** (WNK) WNK1 and WNK4, cause Familial Hyperkalemic Hypertension (FHH) with hypermagnesemia and hypercalciuria³. Moreover, mutations in ubiquitin-ligase complex proteins such as kelch-like-3 (KLHL3) and cullin-3 (CUL3), which control WNK4 stability, are also causative of FHH^{4,5}. The WNK kinases control NCC activity via the **STE20/SPS 1** -related **P**roline- and **A**lanine-rich **K**inase (SPAK) and the **O**xidative **S**tress-**R**esponse kinase **1** (OSR1). SPAK and OSR1 directly phosphorylate NCC at several serine and threonine residues located within the N-terminal tail of the cotransporter^{6,7}.

The activity of the WNK-SPAK kinase pathway and NCC is regulated by various factors including the renin-angiotensin-aldosterone (RAAS) system⁸. Although the DCT expresses the cognate receptors for angiotensin II and aldosterone, recent work suggests that the effect of these hormones on NCC is indirectly mediated via changes in plasma K^+ concentration ($[\text{K}^+]$)^{9,10}. Plasma $[\text{K}^+]$ is proposed to modulate WNK4 activity through changes in DCT membrane voltage and intracellular Cl^- concentration¹¹. Other NCC stimulators such as the β -adrenergic agonist isoproterenol as well as the parathyroid hormone (PTH) are thought to mediate their effects via intracellular cAMP^{12–14}. Recently, the cAMP-dependent protein kinase (PKA) was implicated in the regulation of WNK4, suggesting that cAMP may also act via the WNK/SPAK kinase pathway¹³. However, these studies were mainly performed in heterologous expression systems and it remained unclear whether this and/or additional pathways contribute to the cAMP-dependent regulation of NCC in the native DCT. Some studies suggested that the kinase OSR1 and the extracellular signal-regulated kinase (ERK)1/2 mitogen-activated protein kinase (MAPK) are also involved in the activation of NCC by catecholamines¹⁵ and PTH¹⁶, respectively.

Despite the progress on the elucidation of the role and regulation of the WNK/SPAK/OSR1 kinase pathway, little is known about the phosphatases that counterbalance the action of these kinases. As yet, three protein phosphatases (PP) were suggested to modulate NCC phosphorylation; PP1, PP3 (calcineurin) and PP4. In *Xenopus laevis* oocytes, heterologous co-expression of NCC with PP4 lowered NCC phosphorylation¹⁷. Likewise, pharmacological inhibition of PP1 with calyculin A¹⁸ and of PP3 with tacrolimus^{19,20} increased NCC phosphorylation in various experimental settings. The stimulatory effect of PP3 inhibition on NCC may have important clinical implications. In fact, a common side effect of calcineurin-inhibitor treatment is renal sodium retention and arterial hypertension, which correlates with an enhanced urinary excretion of phosphorylated NCC^{18,21}. Nevertheless, the physiological role of the different phosphatases in the DCT and of the underlying mechanism regulating their function are unclear.

Interestingly, both the catalytic activity and the substrate-specificity of phosphatases are often modulated by the interaction with specific regulatory subunits. We recently found that the endogenous inhibitor 1 (I1) of protein phosphatase 1 is highly expressed in the DCT with strong effects on NCC phosphorylation and arterial blood pressure²². I1 is a small 171 amino acid cytosolic protein encoded by the *Ppp1r1a* gene²³. It is expressed in many organs including the brain, skeletal muscle, and the heart, where it is thought to contribute to neuronal plasticity²⁴, muscle glycogen metabolism²⁵, and cardiac contractility and excitability^{23,26}. Moreover, I1 was implicated in the control of the activity of the Na-K-ATPase in the heart²⁷, while PP1 was found to modulate the inhibitory effect of WNK4 on ROMK in the kidney²⁸. Protein kinase A (PKA) phosphorylates I1 at a threonine residue in position 35 (T35), which activates I1 and makes it a strong and very specific inhibitor of PP1 with an IC₅₀ value of 1nM²⁹. Dephosphorylation of Thr35 by phosphatases such as PP2A and calcineurin (PP3) terminate the inhibitory action of I1²⁶. Interestingly, I1 is critically involved in β -adrenergic and cAMP-dependent signaling in skeletal and heart muscle^{23,26} and I1 deficient mice are partially protected from isoprenaline induced cardiac remodeling and arrhythmia³⁰.

Here, we tested the hypothesis that I1 is also critically involved in the cAMP/PKA-dependent stimulation of NCC phosphorylation. Using a variety of *ex vivo* approaches, we propose a novel signal transduction pathway in which cAMP-dependent

I1 mediates cAMP stimulation of NCC

phosphorylation and activation of I1 mediates the effect of cAMP-elevating hormones on NCC phosphorylation and hence activity.

Materials and Methods

Reagents, cells and antibodies

Unless otherwise stated, reagents were purchased from Sigma Aldrich (Buchs, Switzerland). Calyculin A was purchased from Cell Signaling Technologies (Massachusetts, USA). 8-Br-cAMP, PKI 14-22 amide, myristoylated and H-89 were purchased from Tocris Bioscience (Bristol, UK). Endothall was purchased from EMD Millipore (Billerica, MA, USA).

tNCC, pT53NCC, pT58NCC and pS71NCC antibodies were previously described^{21,22,31}. I1 antibody was purchased from Epitomics (California, USA. Cat. No: 1747-1). The phosphosite-specific antibody recognizing pT35I1 was obtained via affinity purification of serum from rabbits immunized with the phospho-peptide NH₂-CRRRP(pT)PATL-CONH₂ corresponding to mouse I1 (Pineda, Berlin, Germany). The specificity of the antibody was confirmed by immunohistochemistry (supplementary Fig 1). β -actin antibody was purchased from Sigma (Buchs, Cat. No: A5316 Switzerland). Rabbit anti FLAG Antibody was purchased from GenScript (New Jersey, USA, Cat No: A01868). Rabbit anti AQP1 antibody was previously described³². tNCC and pT58NCC antibodies used to detect calyculin A and endothall stimulation of NCC in MDCK type I cells were previously described (references ³³ and ³⁴ respectively). PP1c antibody was purchased from Abcam (Cambridge, UK, Cat No: 53315). Phospho-PKA substrate antibody was purchased from Cell Signaling Technologies (Massachusetts, USA, Cat. No: 9624). OSR1 antibody was purchased from Abcam (Cambridge, UK, Cat. No: 125468).

MDCK type I cells with tetracycline inducible FLAG-tagged NCC were previously characterized³⁵.

Animals

All animal experiments were conducted according to Swiss Laws and approved by the veterinary administration of the Canton of Zurich, Switzerland (License numbers: 213/2015, and 185/2017). Experiments were conducted in male and female I1 deficient mice (I1-KO)²⁴ or wildtype (WT). For automated DCT isolation, mice expressing the enhanced green fluorescent protein (EGFP) in the early segment of the DCT (DCT1) under the parvalbumin promoter (PV-EGFP) were used²². Both transgenic lines and WT animals were kept in a homogenetic C57Bl/6 background.

Mice were maintained in a 12/12 h light/dark cycle and had access to standard chow type 3430 purchased from Provimi-Kliba (Kaiseraugst, Switzerland) and water ad libitum. Animals were age, weight and sex matched for each experimental series.

Kidney slices

Sex, age, and weight matched mice were used for the preparation of kidney slices as described previously¹⁸. To avoid confounding effects on NCC phosphorylation due to unequal dietary intake of K⁺, all mice were food deprived 16 hours prior to the experiment. 280 µm thick slices were incubated in Ringer-type solution for 30 minutes at 30,5°C for equilibration. The K⁺ concentration of the buffer was always 3 mmol/L. Stock solutions of isoproterenol, 3-isobutyl-1-methylxanthine (IBMX), calyculin A, PKI 14-22 amide, myristoylated, and forskolin were prepared in DMSO. Stock solutions of 8-Bromo-cAMP, Na⁺ salt, parathyroid hormone (PTH), norepinephrine (NE), and H-89 were prepared in H₂O. Equal volumes of either DMSO or H₂O were added as control vehicle when needed. After 30 minutes incubation with the drugs or vehicle solutions, slices were snap frozen in liquid nitrogen or immersion fixed with 3% PFA and processed for immunoblotting and histology, respectively. Electron microscopy confirmed that the structural integrity of DCT cells was preserved under the *ex vivo* incubation of the tissue slices (supplementary Fig 2). Further experimental details can be found in the supplementary material and elsewhere¹⁸.

Immunoblotting

Immunoblotting was performed as previously described¹⁸.

Statistics

Unpaired Student's t-test was used to compare two groups. For multiple comparison, one-way or two-way ANOVA followed by Tukey's multiple comparison post-test was performed.

Experimental details of the following methods: yeast two hybrid, immunoprecipitation, immunofluorescence staining and fluorescence quantification, isolated perfused mouse kidney, electron microscopy and automated DCT isolation are included as supplementary material of this manuscript.

Results

cAMP-dependent stimulation of NCC phosphorylation is mediated by PKA

First, we investigated whether an increase in intracellular cAMP levels stimulates NCC phosphorylation in native DCTs via a PKA-dependent pathway. We isolated EGFP-positive early DCT fragments (DCT1) from transgenic mice expressing EGFP under the control of the parvalbumin promoter (PV-EGFP)²². The isolated DCTs were incubated with a cocktail of the adenylate cyclase stimulator forskolin (FSK) (10 μ mol/L) and the phosphodiesterase inhibitor IBMX (100 μ mol/L) in the presence or absence of the PKA inhibitor PKI 14-22. Stimulation with FSK and IBMX triggered a significant increase in the phosphorylation of NCC accompanied with a mild increase in pSPAK-pOSR1 and a marked activation of PKA as monitored using a phospho-PKA substrate antibody (Fig 1). NCC phosphorylation and the anti-phospho-PKA substrate signal substantially diminished upon co-incubation with the PKA inhibitor PKI 14-22 (1 μ mol/L). Under these conditions, the phosphorylation of SPAK and OSR1 remained almost unchanged compared to FSK/IBMX stimulation alone. Incubation of DCTs with 10 μ M PKI 14-22 abolished the phosphorylation of NCC and of the SPAK-OSR1 kinases, indicating an overinhibition of the kinase pathway. Similar to PKI 14-22, the PKA inhibitor (H89) blocked the stimulatory effect of FSK/IBMX on NCC phosphorylation. Surprisingly and for unclear reasons, the effect of H89 was even more pronounced in cAMP-stimulated DCTs than in unstimulated DCTs (supplementary Fig 3).

Genetic ablation of I1 attenuates the cAMP-dependent stimulation of NCC phosphorylation

PKA phosphorylates I1 at position T35 *in vitro*, which renders I1 a potent and highly selective PP1 inhibitor^{29,36}. To test whether I1 is critical for the cAMP-dependent stimulation of NCC, we analyzed kidney slices from WT and I1 deficient mice (I1-KO). Slices were incubated with either FSK, IBMX or the PKA-specific activator 8-Br-cAMP. All agonists strongly increased NCC phosphorylation at Thr 53 (Fig 2 A-C) and at Thr 58 and Ser 71 (Supplementary Fig 4) in kidney slices from WT mice. In contrast, FSK, IBMX, and 8-Br-cAMP had only a small effect on NCC phosphorylation in kidney slices from I1-KO mice (Fig. 2 A-C, and supplementary Fig 4).

Protein phosphatase 1 interacts with and dephosphorylates NCC

Previous studies by us and others showed that all isoforms of the catalytic subunit of PP1 (Ppp1ca, Ppp1cb and Ppp1cc) are highly expressed in mouse²² and rat³⁷ DCTs. Using a yeast-two-hybrid screen on a mouse total kidney library, we found that a NCC fragment comprising the first 133 amino acids of rat NCC interacts with PP1 (Ppp1cb, GI number 161484667) in addition to other known interacting partners (e.g. OSR1³⁸, SPAK³⁹ and Hsp40⁴⁰). To further confirm that PP1 interacts with NCC, co-immunoprecipitation experiments were performed using lysates from MDCK type I cells stably transfected with a tetracycline-inducible FLAG-tagged NCC³⁵. As shown in figure 3A, endogenous PP1 was detected in samples immunoprecipitated with an anti-FLAG antibody but not in samples immunoprecipitated with an anti-AQP1 antibody or in the absence of antibody. Moreover, *in vitro* experiments showed that the PP1 catalytic subunit α is able to dephosphorylate a synthetic peptide corresponding to the N-terminal tail of mouse NCC with a phosphorylated threonine at the position T58 (Fig 3B).

To confirm the functional relevance of PP1 for the regulation of NCC, NCC-expressing MDCK cells were also treated with PP1 and PP2A inhibitors. While the inhibition of PP1 with calyculin A profoundly stimulated NCC phosphorylation, the specific inhibition of PP2A with endothall did not change the phosphorylation of NCC (Fig 3C). Likewise, calyculin A increased NCC phosphorylation in kidney slices from both WT and I1-KO mice to the same extent (Fig 3D), indicating that the effect of calyculin A is downstream of the regulatory action of I1.

Norepinephrin and PTH stimulate NCC phosphorylation in a dose- and I1-dependent manner

It has been previously proposed that norepinephrine (NE) stimulates the phosphorylation of NCC via a PKA-dependent mechanism⁴¹. Moreover, parathyroid hormone (PTH) was shown to activate the adenylate cyclase in the human and rat DCT promoting a strong increase in intracellular cAMP^{12,42}. Using kidney slices from WT and I1-KO mice, we tested whether these two hormones directly stimulate the phosphorylation of NCC in native DCTs and whether this effect depends on I1. As shown in figure 4 A and B, both hormones promote a dose-dependent increase in the phosphorylation of NCC in kidney slices from WT animals. The effect of NE on NCC

phosphorylation was completely abolished in I1-KO mice (Fig 4A). On the other hand, PTH still triggered a residual phosphorylation of NCC in kidney slices from I1-KO animals, although substantially weaker than in WT slices (Fig 4B).

The β -adrenergic stimulation of NCC phosphorylation is mediated by I1

Terker and coworkers suggested that β -adrenergic receptors are instrumental for the stimulation of NCC phosphorylation by catecholamines¹⁵. We hypothesized that the β -adrenergic stimulation of NCC phosphorylation is mediated via I1. To test this hypothesis, kidney slices from WT and I1-KO mice were incubated with the β -adrenergic agonist isoproterenol. Isoproterenol caused a significant rise in NCC phosphorylation in kidney slices from WT mice (Fig 5A) in agreement with previous observations by us¹⁸ and others¹⁵. However, this stimulatory effect was blunted in kidney slices from I1-KO mice, confirming the results with NE stimulation. Similar results were obtained using another *ex-vivo* model, namely the isolated perfused mouse kidney (Fig 5B).

Surprisingly, we did not observe any significant increase in the phosphorylation of SPAK-OSR1 upon stimulation with isoproterenol (Fig 5A). Moreover, when SPAK phosphorylation and activity was clamped at high levels by incubating the kidney slices in a low Cl^- solution (5 mmol/L)¹⁸, the stimulatory effect of isoproterenol on NCC was preserved and clearly additive to the effect of low Cl^- (supplementary figure 5). Moreover, neither the expression of SPAK (Fig 5A) nor of OSR1 (Supplementary figure 6) show any difference between WT and I1-KO kidneys. These findings suggest that at least in our experimental settings, the β -adrenergic stimulation of NCC is largely independent from an activation of the WNK/SPAK-OSR1 pathway.

cAMP promotes I1 phosphorylation at threonine 35 (T35) in native DCTs

To assess whether the activation of PKA promotes I1 phosphorylation in native DCTs, we developed a phosphoform-specific antibody against the PKA-phosphorylation site. This new pT35-I1 antibody recognizes specifically the phosphorylated form of I1 as demonstrated by peptide competition experiments in immunofluorescent studies (supplementary figure 1). Unfortunately, the antibody works only for immunofluorescent studies. Therefore, we assessed the phosphorylation levels of I1 by immunohistochemistry. Consecutive cryosections obtained from kidney slices incubated *ex vivo* either with vehicle or isoproterenol were stained with antibodies

against total I1 (tI1), pT35I1, tNCC and pT53NCC (Fig 6) and the staining intensities in DCTs were then quantified using ImageJ software as described in the material and method section. As previously reported²², I1 protein was found to be highly abundant in DCTs and in thick ascending limbs of Henle's loop (TAL) (Fig 6A). In contrast to total I1, pT35I1 was barely detectable in DCTs in vehicle treated kidney slices. However, the signal for pT35I1 and also pT53NCC significantly increased in DCTs in kidney slices stimulated with isoproterenol (Fig 6A and B). Strikingly, the phosphorylation of I1 and NCC showed a strong linear correlation (Fig 6B). Of notice, both the total and the phosphorylated form of I1 were mainly seen at the apical cell surface of DCTs and hence in proximity to NCC (Fig 6A and C).

Discussion

The DCT is the target for several cAMP-elevating hormones including β -adrenergic agonists, PTH and vasopressin¹². These hormones are known to activate the DCT-specific NaCl cotransporter NCC but the involved signal transduction pathways remained poorly defined. In the present study, we used a set of *ex vivo* approaches to reveal a complete signal transduction pathway by which cAMP-elevating hormones, via PKA, I1 and PP1 control NCC phosphorylation and hence activity.

In our studies, we tested the effect of two physiologically relevant hormones, namely norepinephrine and PTH. Both hormones strongly stimulated NCC phosphorylation in a dose-dependent manner in a range from 0.1 nmol/L to 100 nmol/L. For norepinephrine, this range matches well with the reference range of normal plasma norepinephrine concentrations in humans (i.e. 0.83-10 nmol/L)⁴³. For PTH, this range is above physiological levels (20-65 ng/L, ~2-6.5 pmol/L)⁴⁴. However, the PTH applied to native tissue elicited effects on NCC already at concentrations that were far below those reported in the literature (100 nmol/L) to activate NCC and TRPV5^{16,45} and to downregulate NaPi2a⁴⁶ in cell systems and tissue slices, respectively. It is also important to consider that PTH is a peptide hormone that likely penetrates less efficiently into the tissue slices than the much smaller catecholamines. Moreover, the high levels of peptidases in the kidney slices (e.g. in the brush border of proximal tubules) may rapidly degrade PTH to inactive metabolites. Independent, from these possible technical hurdles, the data clearly indicate that both hormones are able to elicit a graded response of NCC phosphorylation. At least for norepinephrine, this graded response occurs in the range of physiological and pathophysiological plasma norepinephrine variations and may hence contribute to altered renal sodium reabsorption in response to changed sympathetic tone.

Several studies already suggested that cAMP-dependent activation of PKA contributes to the hormonal regulation of NCC^{13,15,41,47-49}. Nevertheless, as pointed out by Mutig et al. direct experimental support for the role of cAMP and PKA for the control of NCC activity in native DCTs had been limited probably due to the difficulty to establish readily available and suitable DCT cell models⁴⁸. Now, using isolated mouse DCTs and kidney slices incubated *ex vivo* with forskolin and IBMX in the absence or presence of the PKA inhibitors PKI 14-22 and H-89, we provide compelling evidence that cAMP and PKA modify NCC activity in the native DCT. I1 is a direct target for PKA,

which phosphorylates I1 at a threonine in position 53 (pT35I1) and converts it into a potent and selective inhibitor of PP1²⁹. Consistent with an activation of the cAMP/PKA pathway in native DCTs, we observed a profound stimulation of I1 phosphorylation at the consensus PKA site (pT35) in response to isoproterenol stimulation. The I1 phosphorylation strongly correlated with the level of NCC phosphorylation suggesting that they are functionally linked. Interestingly, I1 appears to be barely phosphorylated at the PKA site (T35) in DCTs of vehicle-treated kidney slices suggesting that I1-dependent NCC regulation plays a significant role in response to hormonal stimuli but not under resting conditions.

In vitro kinase assays and experiments in heterologous expression systems suggested that PKA exerts its effects on NCC via the classical KHL3-WNK4-SPAK pathway. PKA-mediated phosphorylation of KHL3 at S433 decreases KHL3-dependent ubiquitination and degradation of WNK4⁴⁷. Likewise, PKA phosphorylates WNK4 at multiple sites including S64 and S1169, which finally promotes WNK4-dependent phosphorylation and activation of SPAK¹³. PP1 was shown to modulate the phosphorylation levels of both WNK4²⁸ and SPAK⁵⁰. Studies on the regulation of the Na-K-2Cl cotransporter NKCC1, which is structurally related to NCC, suggested that PP1 binds to the N-terminal tail of NKCC1 in direct proximity to SPAK to dephosphorylate both SPAK and NKCC1⁵⁰. NCC lacks the amino acid motif mediating the binding of PP1 to NKCC1⁵⁰. Nevertheless, our yeast-two-hybrid and co-immunoprecipitation data suggest that PP1 and NCC do also interact and might be linked in a signaling complex that may involve also WNK4 and SPAK/OSR1. Therefore, it is conceivable that I1 and PP1 may control NCC activity directly via NCC-dephosphorylation and/or indirectly via controlling WNK4 and SPAK/OSR1 phosphorylation. However, neither in the current nor in our previous studies, we observed significant evidence for an involvement of I1 in SPAK/OSR1 regulation. The abundance and subcellular localization of total-SPAK, total-OSR1 (this study) and pSPAK/pOSR1 were similar in the kidneys and DCTs of wildtype and I1-KO mice²². Moreover, FSK/IBMX and isoproterenol had no significant effects on SPAK/OSR1 phosphorylation in isolated DCTs (Fig 1) and in kidney slices (Fig 5), respectively. Likewise, incubation of the kidney slices in a low Cl⁻-solution, which clamps SPAK/OSR1 activity at high levels¹⁸ did not block the stimulatory effect of isoproterenol on NCC phosphorylation (suppl. Fig 5). Nevertheless, these negative results do not

formally exclude some activation of the WNK4/SPAK/OSR1 pathway. In fact, we consistently observed slight, but never statistically significant, increases in pSPAK/OSR1 immunoreactivities in tissue samples treated with FSK/IBMX and isoproterenol. Moreover, previous studies on heterologous expression systems linked SPAK to the cAMP/PKA-dependent NCC regulation¹³, while studies on knockout mouse models implicated OSR1 (but not SPAK) in the catecholamine-dependent control of NCC¹⁵. Part of these discrepancies may reflect the different experimental settings (e.g. in vitro, ex vivo, in vivo) and compounds used, but they may also indicate some redundancies in the signaling pathways, by which cAMP-elevating hormones stimulate NCC activity. In line with this view, we consistently observed some residual cAMP-dependent stimulation of NCC phosphorylation in kidneys of I1-KO mice in response to forskolin/IBMX and in particular in response to PTH. In contrast, the effect of catecholamines (isoproterenol and norepinephrine) on NCC phosphorylation appeared to depend almost exclusively on the presence of I1. A possible explanation for these differences might be a compartmentalization of the cAMP signaling pathways. In fact, cAMP reporter assays provided evidence for a spatial and temporal control of cAMP dynamics due to the presence of local micro-domains with proteins producing and degrading cAMP⁵¹, which allow circumscribed effects independent from cAMP levels outside these microdomains⁵². Thus, the hormone-induced cAMP/PKA-dependent activation of NCC may involve several redundant pathways including the previously characterized WNK4, SPAK and OSR1 kinase pathways^{15,35,48,53}. The current study adds I1 as an important additional regulator and suggests that in addition to the NCC-controlling kinases also the phosphatases are tightly regulated. Figure 7 shows the proposed signaling model that we believe best explains the current observations in the context of prior knowledge.

Aside from these novel insights into the molecular mechanism controlling NCC function, our findings may have some clinical implications. Inappropriately high sympathetic activity is thought to contribute to cardiovascular diseases including cardiac arrhythmia, cardiac failure, and arterial hypertension⁵⁴. Previous studies already implicated I1 in the β -adrenergic response of the heart modulating cardiac contractility⁵⁵, excitability²², and remodeling²³. The present study extends these observations to the kidney and shows that I1 is also critically involved in the renal response to catecholamines. Our data indicate that catecholamines increase the

phosphorylation of I1 at the PKA-consensus site T35, which convert I1 into a potent inhibitor of PP1-dependent NCC dephosphorylation. This finally increases NCC phosphorylation as observed in the present and several other^{15,41,56} but not all⁵⁷ previous studies and may contribute to norepinephrine-induced salt sensitive hypertension⁵⁸. Interestingly, the pT35 site of I1 is dephosphorylated by PP3 (calcineurin)²³. Immunosuppressive therapy with calcineurin inhibitors such as tacrolimus and cyclosporine A is often complicated by the development of arterial hypertension, which was suggested to be linked to renal Na⁺ retention due to an activation of NCC¹⁹. It is tempting to speculate that at least part of these effects are also mediated via I1. Future in vivo studies, will have to address the relevance of renal I1 for catecholamine- and calcineurin-induced arterial hypertension.

In summary, the present study identified the inhibitor 1 (I1) of protein phosphatase 1 as a central regulatory element in the signal transduction cascade that mediates the stimulatory effects of cAMP on the thiazide-sensitive NaCl cotransporter. I1 may represent an interesting point of convergence for different kinase and phosphatase pathways in the DCT contributing to the regulation of NCC in health and disease. Given its relevance for both the cardiac and renal response to β -adrenergic stimulation, I1 might also be an interesting drug target for the treatment of cardiovascular diseases, including arterial hypertension.

Author contributions:

DP, RAF, DLC and JL conceived and designed the study. DP, AW, SM, JC, LLR, FR, JRM, NF, RAF and DLC collected, analyzed and interpret the data. DP, RAF and JL wrote the manuscript. All authors approved the final version of the manuscript.

SM and AW contributed equally to this study.

Acknowledgments

The authors thank Monique Carrel, Michèle Heidemeyer, Shunmugam Nagarajan, and Tina Drejer for their excellent technical assistance and Adisa Trnjanin-Hadzic and Erich Brunner for their help with immunoprecipitations and biosorting, respectively.

Grants

David Penton is a fellow of the Program on Integrative Kidney Physiology and Pathophysiology (IKPP2) funded by the European Union's Seventh Framework Program for research, technological development and demonstration under grant agreement no 608847. Johannes Loffing is supported by research funds from the Swiss National Centre for Competence in Research "Kidney.CH", by project grants from the Swiss National Science Foundation (310030_143929/1) and by the COST Action ADMIRE BM1301. Funding to Robert Fenton is provided by the Danish Medical Research Foundation, the Lundbeck Foundation, the Novo Nordisk Foundation and Aarhus University Research Foundation.

Disclosures

Authors have nothing to disclose

Supplemental material Table of content:

- Detailed methods
- Supplementary Figure 1: Assessment of the specificity of the pT35I1 antibody by immunohistochemistry
- Supplementary Figure 2: Assessment of DCT integrity in kidney slices via electron microscopy
- Supplementary Figure 3: Inhibition of cAMP-dependent phosphorylation of NCC by the PKA inhibitor H-89
- Supplementary Figure 4: Stimulation of NCC phosphorylation at T58 and S71 with cAMP elevating agents
- Supplementary Figure 5: Effect of low Cl⁻ on the stimulation of NCC and SPAK-OSR1 phosphorylation by isoproterenol in kidney slices of WT mouse
- Supplementary Figure 6: Expression of OSR1 in WT and I1-KO mice
- Supplementary table 1
- Supplementary table 2
- References

References

1. Subramanya AR, Ellison DH: Distal convoluted tubule. *Clin. J. Am. Soc. Nephrol.* 9: 2147–63, 2014
2. Riveira-Munoz E, Chang Q, Bindels RJ, Devuyst O: Gitelman's syndrome: Towards genotype-phenotype correlations? *Pediatr. Nephrol.* 22: 326–332, 2007
3. Murthy M, Kurz T, O'Shaughnessy KM: WNK signalling pathways in blood pressure regulation. *Cell. Mol. Life Sci.* 74: 1261–1280, 2017
4. Shibata S, Zhang J, Puthumana J, Stone KL, Lifton RP: Kelch-like 3 and Cullin 3 regulate electrolyte homeostasis via ubiquitination and degradation of WNK4. *Proc. Natl. Acad. Sci. U. S. A.* 110: 7838–43, 2013
5. Boyden LM, Choi M, Choate KA, Nelson-Williams CJ, Farhi A, Toka HR, Tikhonova IR, Bjornson R, Mane SM, Colussi G, Lebel M, Gordon RD, Semmekrot BA, Poujol A, Välimäki MJ, De Ferrari ME, Sanjad SA, Gutkin M, Karet FE, Tucci JR, Stockigt JR, Keppler-Noreuil KM, Porter CC, Anand SK, Whiteford ML, Davis ID, Dewar SB, Bettinelli A, Fadrowski JJ, Belsha CW, Hunley TE, Nelson RD, Trachtman H, Cole TRP, Pinsk M, Bockenhauer D, Shenoy M, Vaidyanathan P, Foreman JW, Rasoulpour M, Thameem F, Al-Shahrouri HZ, Radhakrishnan J, Gharavi AG, Goilav B, Lifton RP: Mutations in kelch-like 3 and cullin 3 cause hypertension and electrolyte abnormalities. *Nature* 482: 98–102, 2012
6. Yang S-S, Fang Y-W, Tseng M-H, Chu P-Y, Yu I-S, Wu H-C, Lin S-W, Chau T, Uchida S, Sasaki S, Lin Y-F, Sytwu H-K, Lin S-H: Phosphorylation regulates NCC stability and transporter activity in vivo. *J. Am. Soc. Nephrol.* 24: 1587–97, 2013
7. Hadchouel J, Ellison DH, Gamba G: Regulation of Renal Electrolyte Transport by WNK and SPAK-OSR1 Kinases. *Annu. Rev. Physiol.* 78: 367–389, 2016
8. Rojas-Vega L, Gamba G: Mini-review: regulation of the renal NaCl cotransporter by hormones. *Am. J. Physiol. Renal Physiol.* 310: F10–4, 2016
9. Terker AS, Yarbrough B, Ferdaus MZ, Lazelle RA, Erspamer KJ, Meermeier NP, Park HJ, McCormick JA, Yang C-L, Ellison DH: Direct and Indirect Mineralocorticoid Effects Determine Distal Salt Transport. *J. Am. Soc. Nephrol.* 1–10, 2015
10. Czogalla J, Vohra T, Penton D, Kirschmann M, Craigie E, Loffing J: The mineralocorticoid receptor (MR) regulates ENaC but not NCC in mice with random MR deletion. *Pflügers Arch. Eur. J. Physiol.* 468: 849–58, 2016
11. Terker AS, Zhang C, McCormick JA, Lazelle RA, Zhang C, Meermeier NP, Siler DA, Park HJ, Fu Y, Cohen DM, Weinstein AM, Wang W-H, Yang C-L, Ellison DH: Potassium Modulates Electrolyte Balance and Blood Pressure through Effects on Distal Cell Voltage and Chloride. *Cell Metab.* 21: 39–50, 2015
12. Morel F: Sites of hormone action in the mammalian nephron. *Am. J. Physiol.* 240: F159–64, 1981
13. Castañeda-Bueno M, Arroyo JP, Zhang J, Puthumana J, Yarborough O, Shibata S, Rojas-

- Vega L, Gamba G, Rinehart J, Lifton RP: Phosphorylation by PKC and PKA regulate the kinase activity and downstream signaling of WNK4. *Proc. Natl. Acad. Sci. U. S. A.* 114: E879–E886, 2017
14. Cheng L, Wu Q, Kortenoeven MLA, Pisitkun T, Fenton RA: A Systems Level Analysis of Vasopressin-mediated Signaling Networks in Kidney Distal Convoluted Tubule Cells. *Sci. Rep.* 5: 12829, 2015
 15. Terker AS, Yang C-L, McCormick J a, Meermeier NP, Rogers SL, Grossmann S, Trompf K, Delpire E, Loffing J, Ellison DH: Sympathetic stimulation of thiazide-sensitive sodium chloride cotransport in the generation of salt-sensitive hypertension. *Hypertension* 64: 178–84, 2014
 16. Ko B, Cooke LL, Hoover RS: Parathyroid hormone (PTH) regulates the sodium chloride cotransporter via Ras guanyl releasing protein 1 (Ras-GRP1) and extracellular signal-regulated kinase (ERK)1/2 mitogen-activated protein kinase (MAPK) pathway. *Transl. Res.* 158: 282–289, 2011
 17. Gamba G: Regulation of the renal Na⁺-Cl⁻ cotransporter by phosphorylation and ubiquitylation. *Am. J. Physiol. Renal Physiol.* 303: F1573-83, 2012
 18. Penton D, Czogalla J, Wengi A, Himmerkus N, Loffing-Cueni D, Carrel M, Rajaram RD, Staub O, Bleich M, Schweda F, Loffing J: Extracellular K(+) rapidly controls NaCl cotransporter phosphorylation in the native distal convoluted tubule by Cl(-) - dependent and independent mechanisms. *J. Physiol.* 594: 6319–6331, 2016
 19. Hoorn EJ, Walsh SB, McCormick JA, Fürstenberg A, Yang C-L, Roeschel T, Paliege A, Howie AJ, Conley J, Bachmann S, Unwin RJ, Ellison DH: The calcineurin inhibitor tacrolimus activates the renal sodium chloride cotransporter to cause hypertension. *Nat. Med.* 17: 1304–9, 2011
 20. Shoda W, Nomura N, Ando F, Mori Y, Mori T, Sohara E, Rai T, Uchida S: Calcineurin inhibitors block sodium-chloride cotransporter dephosphorylation in response to high potassium intake. *Kidney Int.* 91: 402–411, 2017
 21. Sorensen M V, Grossmann S, Roesinger M, Gresko N, Todkar AP, Barmettler G, Ziegler U, Odermatt A, Loffing-Cueni D, Loffing J: Rapid dephosphorylation of the renal sodium chloride cotransporter in response to oral potassium intake in mice. *Kidney Int.* 83: 811–24, 2013
 22. Picard N, Trompf K, Yang C-L, Miller RL, Carrel M, Loffing-Cueni D, Fenton RA, Ellison DH, Loffing J: Protein phosphatase 1 inhibitor-1 deficiency reduces phosphorylation of renal NaCl cotransporter and causes arterial hypotension. *J. Am. Soc. Nephrol.* 25: 511–22, 2014
 23. Wittköpper K, Dobrev D, Eschenhagen T, El-Armouche A: Phosphatase-1 inhibitor-1 in physiological and pathological β -adrenoceptor signalling. *Cardiovasc. Res.* 91: 392–401, 2011
 24. Allen PB, Hvalby O, Jensen V, Errington ML, Ramsay M, Chaudhry F a, Bliss T V, Storm-Mathisen J, Morris RG, Andersen P, Greengard P: Protein phosphatase-1 regulation in the induction of long-term potentiation: heterogeneous molecular mechanisms. *J.*

- Neurosci.* 20: 3537–43, 2000
25. Nimmo GA, Cohen P: The regulation of glycogen metabolism. Purification and characterisation of protein phosphatase inhibitor-1 from rabbit skeletal muscle. *Eur. J. Biochem.* 87: 341–51, 1978
 26. Nicolaou P, Hajjar RJ, Kranias EG: Role of protein phosphatase-1 inhibitor-1 in cardiac physiology and pathophysiology. *J. Mol. Cell. Cardiol.* 47: 365–71, 2009
 27. El-Armouche A, Wittköpper K, Fuller W, Howie J, Shattock MJ, Pavlovic D: Phospholemman-dependent regulation of the cardiac Na/K-ATPase activity is modulated by inhibitor-1 sensitive type-1 phosphatase. *FASEB J.* 25: 4467–75, 2011
 28. Lin D-H, Yue P, Rinehart J, Sun P, Wang Z, Lifton R, Wang W-H: Protein phosphatase 1 modulates the inhibitory effect of With-no-Lysine kinase 4 on ROMK channels. *Am. J. Physiol. Renal Physiol.* 303: F110-9, 2012
 29. Endo S, Zhou X, Connor J, Wang B, Shenolikar S: Multiple structural elements define the specificity of recombinant human inhibitor-1 as a protein phosphatase-1 inhibitor. *Biochemistry* 35: 5220–5228, 1996
 30. El-Armouche A, Wittköpper K, Degenhardt F, Weinberger F, Didié M, Melnychenko I, Grimm M, Peeck M, Zimmermann WH, Unsöld B, Hasenfuss G, Dobrev D, Eschenhagen T: Phosphatase inhibitor-1-deficient mice are protected from catecholamine-induced arrhythmias and myocardial hypertrophy. *Cardiovasc. Res.* 80: 396–406, 2008
 31. Wagner CA, Loffing-Cueni D, Yan Q, Schulz N, Fakitsas P, Carrel M, Wang T, Verrey F, Geibel JP, Giebisch G, Hebert SC, Loffing J: Mouse model of type II Bartter's syndrome. II. Altered expression of renal sodium- and water-transporting proteins. *Am. J. Physiol. Renal Physiol.* 294: F1373-80, 2008
 32. Terris J, Ecelbarger CA, Nielsen S, Knepper MA: Long-term regulation of four renal aquaporins in rats. *Am. J. Physiol. Physiol.* 271: F414–F422, 1996
 33. Kim GH, Masilamani S, Turner R, Mitchell C, Wade JB, Knepper MA: The thiazide-sensitive Na-Cl cotransporter is an aldosterone-induced protein. *Proc. Natl. Acad. Sci. U. S. A.* 95: 14552–14557, 1998
 34. Pedersen NB, Hofmeister M V, Rosenbaek LL, Nielsen J, Fenton R a: Vasopressin induces phosphorylation of the thiazide-sensitive sodium chloride cotransporter in the distal convoluted tubule. *Kidney Int.* 78: 160–9, 2010
 35. Rosenbaek LL, Kortenoeven MLA, Aroankins TS, Fenton RA: Phosphorylation decreases ubiquitylation of the thiazide-sensitive cotransporter NCC and subsequent clathrin-mediated endocytosis. *J. Biol. Chem.* 289: 13347–61, 2014
 36. Huang FL, Glinsmann WH: Separation and characterization of two phosphorylase phosphatase inhibitors from rabbit skeletal muscle. *Eur. J. Biochem.* 70: 419–26, 1976
 37. Lee JW, Chou C-L, Knepper MA: Deep Sequencing in Microdissected Renal Tubules Identifies Nephron Segment-Specific Transcriptomes. *J. Am. Soc. Nephrol.* 26: 2669–77, 2015
 38. Richardson C, Rafiqi FH, Karlsson HKR, Moleleki N, Vandewalle A, Campbell DG, Morrice

- NA, Alessi DR: Activation of the thiazide-sensitive Na⁺-Cl⁻ cotransporter by the WNK-regulated kinases SPAK and OSR1. *J. Cell Sci.* 121: 675–84, 2008
39. Piechotta K, Lu J, Delpire E: Cation chloride cotransporters interact with the stress-related kinases Ste20-related proline-alanine-rich kinase (SPAK) and oxidative stress response 1 (OSR1). *J. Biol. Chem.* 277: 50812–50819, 2002
40. Donnelly BF, Needham PG, Snyder AC, Roy A, Khadem S, Brodsky JL, Subramanya AR: Hsp70 and Hsp90 multichaperone complexes sequentially regulate thiazide-sensitive cotransporter endoplasmic reticulum-associated degradation and biogenesis. *J. Biol. Chem.* 288: 13124–13135, 2013
41. Mu S, Shimosawa T, Ogura S, Wang H, Uetake Y, Kawakami-Mori F, Marumo T, Yatomi Y, Geller DS, Tanaka H, Fujita T: Epigenetic modulation of the renal β -adrenergic-WNK4 pathway in salt-sensitive hypertension. *Nat. Med.* 17: 573–80, 2011
42. Chabardes D, Gagnan-Brunette M, Imbert-Teboul M, Gontcharevskaja O, Montégut M, Clique A, Morel F: Adenylate cyclase responsiveness to hormones in various portions of the human nephron. *J. Clin. Invest.* 65: 439–448, 1980
43. Duncan MW, Compton P, Lazarus L, Smythe GA: Measurement of Norepinephrine and 3,4-Dihydroxyphenylglycol in Urine and Plasma for the Diagnosis of Pheochromocytoma. *N. Engl. J. Med.* 319: 136–142, 1988
44. Insogna KL: Primary Hyperparathyroidism. *N. Engl. J. Med.* 379: 1050–1059, 2018
45. Hoover RS, Tomilin V, Hanson LN, Pochynyuk O, Ko B: PTH Modulation of NCC Activity Regulates TRPV5 Calcium Reabsorption. *Am. J. Physiol. - Ren. Physiol.* ajprenal.00323.2015, 2015
46. Bacic D, Schulz N, Biber J, Kaissling B, Murer H, Wagner CA: Involvement of the MAPK-kinase pathway in the PTH-mediated regulation of the proximal tubule type IIa Na⁺/Picotransporter in mouse kidney. *Pflugers Arch. Eur. J. Physiol.* 446: 52–60, 2003
47. Yoshizaki Y, Mori Y, Tsuzaki Y, Mori T, Nomura N, Wakabayashi M, Takahashi D, Zeniya M, Kikuchi E, Araki Y, Ando F, Isobe K, Nishida H, Ohta A, Susa K, Inoue Y, Chiga M, Rai T, Sasaki S, Uchida S, Sohara E: Impaired degradation of WNK by Akt and PKA phosphorylation of KLHL3. *Biochem. Biophys. Res. Commun.* 467: 229–234, 2015
48. Mutig K, Saritas T, Uchida S, Kahl T, Borowski T, Paliege A, Böhlick A, Bleich M, Shan Q, Bachmann S: Short-term stimulation of the thiazide-sensitive Na⁺-Cl⁻ cotransporter by vasopressin involves phosphorylation and membrane translocation. *Am. J. Physiol. Renal Physiol.* 298: F502-9, 2010
49. Gonzalez-Nunez D, Morales-Ruiz M, Leivas A, Hebert SC, Poch E: In vitro characterization of aldosterone and cAMP effects in mouse distal convoluted tubule cells. *Am J Physiol Ren. Physiol* 286: F936-44, 2004
50. Gagnon KB, Delpire E: Multiple pathways for protein phosphatase 1 (PP1) regulation of Na-K-2Cl cotransporter (NKCC1) function: The N-terminal tail of the Na-K-2Cl cotransporter serves as a regulatory scaffold for Ste20-related proline/alanine-rich kinase (SPAK) and PP1. *J. Biol. Chem.* 285: 14115–14121, 2010

51. Baillie GS: Compartmentalized signalling: Spatial regulation of cAMP by the action of compartmentalized phosphodiesterases. *FEBS J.* 276: 1790–1799, 2009
52. Averaimo S, Assali A, Ros O, Couvet S, Zagar Y, Genescu I, Rebsam A, Nicol X: A plasma membrane microdomain compartmentalizes ephrin-generated cAMP signals to prune developing retinal axon arbors. *Nat. Commun.* 7: 1–12, 2016
53. Saritas T, Borschewski A, McCormick J a, Paliege A, Dathe C, Uchida S, Terker A, Himmerkus N, Bleich M, Demaretz S, Laghmani K, Delpire E, Ellison DH, Bachmann S, Mutig K: SPAK differentially mediates vasopressin effects on sodium cotransporters. *J. Am. Soc. Nephrol.* 24: 407–18, 2013
54. Manolis AJ, Poulimenos LE, Kallistratos MS, Gavras I, Gavras H: Sympathetic overactivity in hypertension and cardiovascular disease. *Curr. Vasc. Pharmacol.* 12: 4–15, 2014
55. Carr AN, Schmidt AG, Suzuki Y, del Monte F, Sato Y, Lanner C, Breeden K, Jing S, Allen PB, Greengard P, Yatani A, Hoit BD, Grupp IL, Hajjar RJ, DePaoli-Roach AA, Kranias EG: Type 1 phosphatase, a negative regulator of cardiac function. *Mol. Cell. Biol.* 22: 4124–35, 2002
56. Walsh KR, Kuwabara JT, Shim JW, Wainford RD: Norepinephrine-evoked salt-sensitive hypertension requires impaired renal sodium chloride cotransporter activity in Sprague-Dawley rats. *Am. J. Physiol. - Regul. Integr. Comp. Physiol.* 310: R115–R124, 2016
57. Uchida S, Chiga M, Sohara E, Rai T, Sasaki S: Does a β 2-adrenergic receptor-WNK4-Na-Cl co-transporter signal cascade exist in the in vivo kidney? *Nat. Med.* 18: 1324-5; author reply 1325-7, 2012
58. Fujita T: Mechanism of salt-sensitive hypertension: focus on adrenal and sympathetic nervous systems. *J. Am. Soc. Nephrol.* 25: 1148–55, 2014

Figure 1: PKA activation stimulates NCC phosphorylation in native DCTs. Left panel represents a typical immunoblot of isolated DCTs treated with vehicle, 10 $\mu\text{mol/L}$ FSK + 100 $\mu\text{mol/L}$ IBMX, FSK / IBMX + 1 $\mu\text{mol/L}$ PKI 14-22 and FSK / IBMX + 10 $\mu\text{mol/L}$ PKI 14-22 . The activity of PKA was monitored using a phospho-PKA substrate antibody. Each lane corresponds to 400 DCT fragments. On the right, the densitometric analysis of pT53NCC/tNCC and pSPAK-pOSR1/tSPAK from 4 independent experiments ("n" in brackets) normalized to control vehicle group (red line) is represented. Error bars represent the standard error of the mean (SEM). * $p < 0.05$ compared to control vehicle condition and assessed by one-way ANOVA followed by Tukey's multiple comparisons test.

Figure 2: PKA stimulation of NCC phosphorylation is impaired in I1-KO mice. Representative immunoblots showing the effect of **(A)** IBMX (100 $\mu\text{mol/L}$), **(B)** forskolin (10 $\mu\text{mol/L}$) and **(C)** 8-Br-cAMP (10 $\mu\text{mol/L}$) on NCC phosphorylation at position T53 in WT and I1-KO kidney slices. Bar charts represent the densitometric quantification of pT53NCC/tNCC normalized to control vehicle of each genotype from 6-9 slices ("n" in brackets) from 2-3 mice. Error bars represent the standard error of the mean (SEM). * $p < 0.05$, ** $p < 0.01$, *** $p < 0.001$, **** $p < 0.0001$ assessed by two-way ANOVA followed by Tukey's multiple comparison post-test.

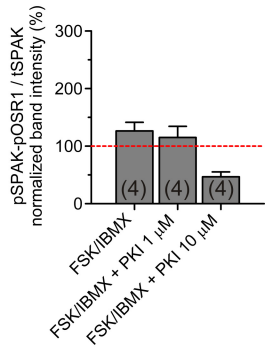
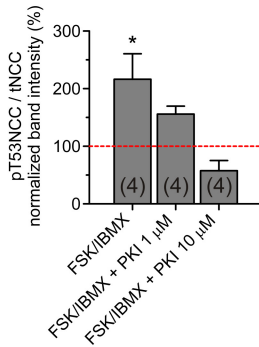
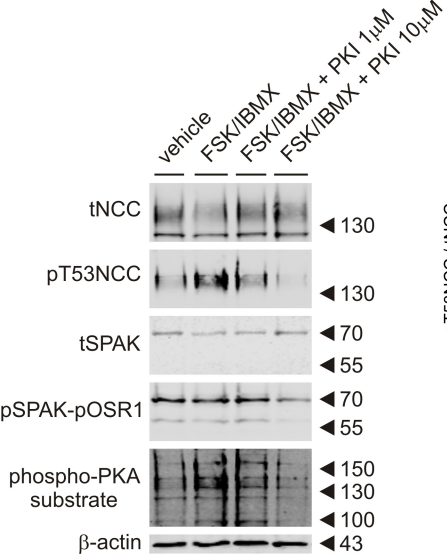
Figure 3: Protein Phosphatase 1 interacts with NCC and dephosphorylates it. **A:** FLAG IP pull down of NCC (left) and the catalytic subunit of PP1 (PP1c) (right). Unrelated anti-AQP1 antibody as well as no antibody were used as negative control. **B:** *in vitro* dephosphorylation of biotinylated pT58-mNCC peptide by PP1. **C:** Changes in NCC phosphorylation at T58 in MDCK type I cells with tetracycline inducible FLAG-tagged NCC expression upon treatment with calyculin A (left panel) or specific PP2A inhibitor endothall (right panel). Graph represents the densitometric quantification of immunoblots from 2 independent experiments * $p < 0.05$ by one-way ANOVA followed by Tukey's multiple comparisons test. **D:** Changes in NCC phosphorylation upon treatment of WT and I1-KO mouse kidney slices with Calyculin A (20 nmol/L). Bar charts represent the densitometric quantification of pT53NCC/tNCC from 6 slices (in brackets) normalized to control vehicle of each genotype (2 mice per group). Error bars represent the standard error of the mean (SEM). ns: non-significant; **** $p < 0.0001$ assessed by two-way ANOVA followed by Tukey's multiple comparison post-test.

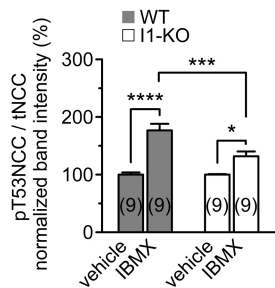
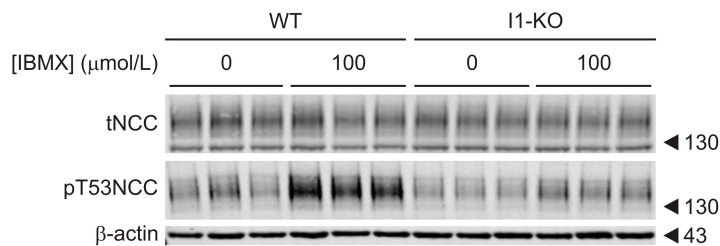
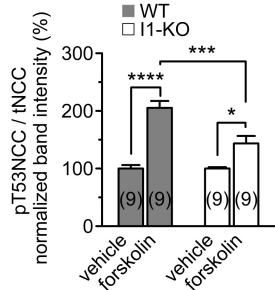
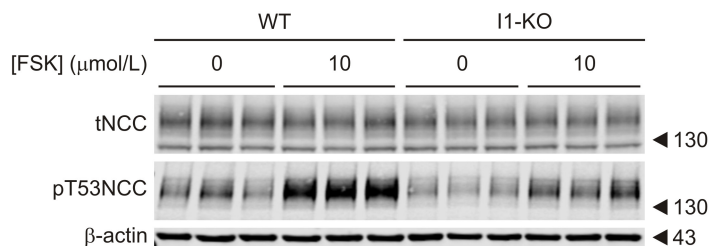
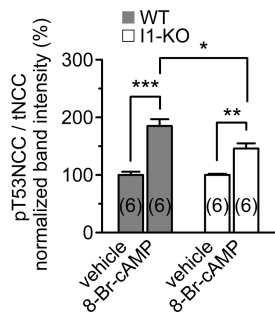
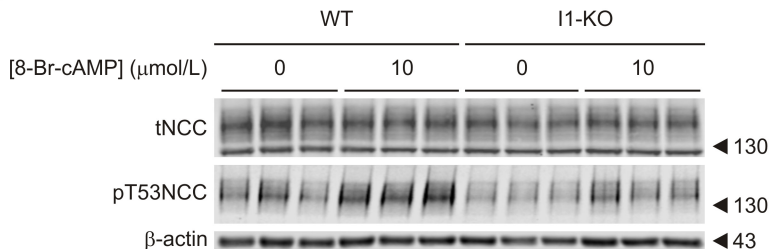
Figure 4: I1 mediates the effect of cAMP-increasing hormones on NCC phosphorylation. Dose-response effect of (A) Norepinephrine (NE) and (B) parathyroid hormone (PTH) on NCC phosphorylation (T53) in WT and I1-KO mouse kidney slices. Graphs represent the densitometric quantification of pT53NCC/tNCC normalized to control vehicle of each genotype (red line). The number of slices assayed from 1 (NE) or 2 (PTH) mice per genotype are in brackets. Error bars represent the standard error of the mean (SEM). Stars denote statistically significant differences (* $p < 0.05$, ** $p < 0.01$, **** $p < 0.0001$) between the two genotypes for the same hormone concentration assessed by unpaired Student's t-test.

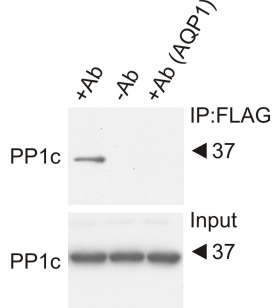
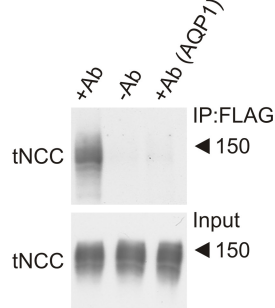
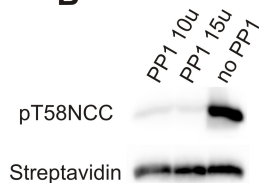
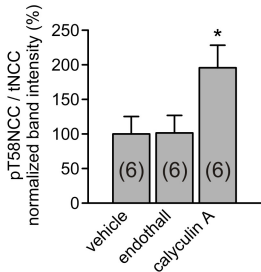
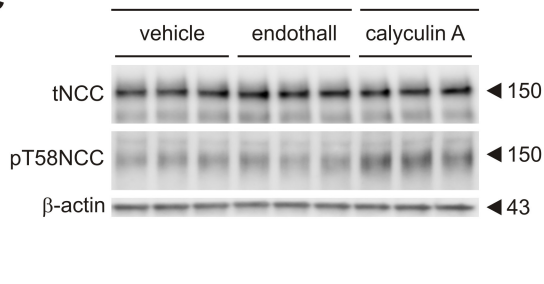
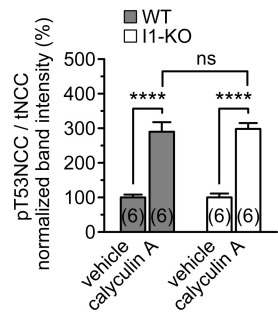
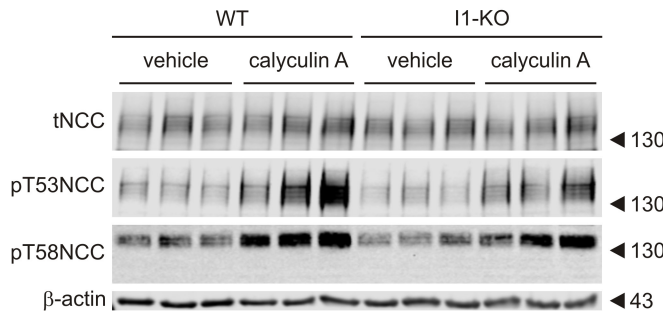
Figure 5: The β -adrenergic stimulation of NCC phosphorylation is impaired in I1-KO mice. **A:** Dose-response effect of β -adrenergic agonist isoproterenol on the phosphorylation of NCC (T53), SPAK and OSR1 in WT and I1-KO kidney slices. Graphs represent the densitometric quantification of the phosphorylation of pT53NCC/tNCC and pSPAK-pOSR1/tSPAK normalized to vehicle control of each genotype from 3-15 slices (in brackets) (1-5 mice), Stars represent statistical significance (* $p < 0.05$, ** $p < 0.01$, **** $p < 0.0001$) of the comparison between the two genotypes for the same concentration of isoproterenol assessed by unpaired Student's t-test. **B:** β -adrenergic stimulation of NCC phosphorylation in isolated perfuse mouse kidneys. Bar charts represent the densitometric quantification of pT53NCC/tNCC normalized to control vehicle of each genotype in 4-5 mice / experiment ("n" in brackets). ns: non-significant; ** $p < 0.01$ assessed by two-way ANOVA followed by Tukey's multiple comparison post-test. Error bars represent the standard error of the mean (SEM).

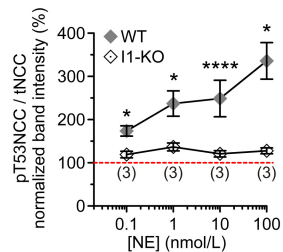
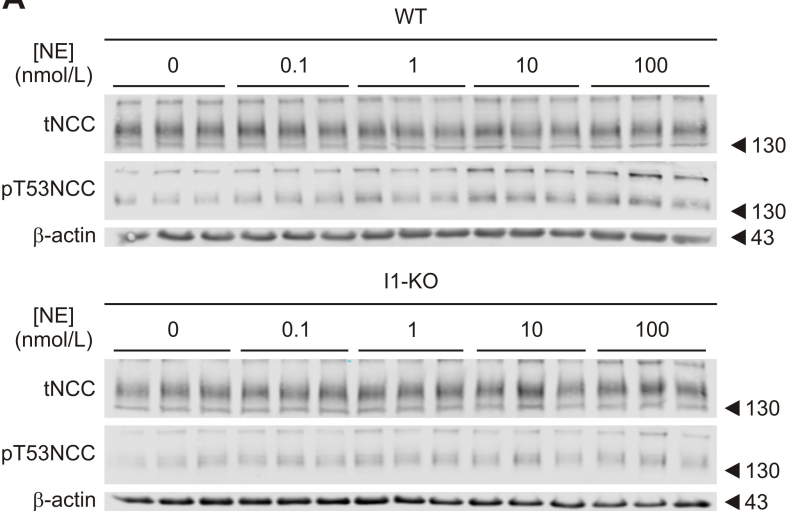
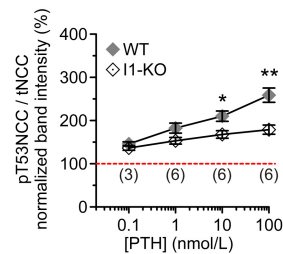
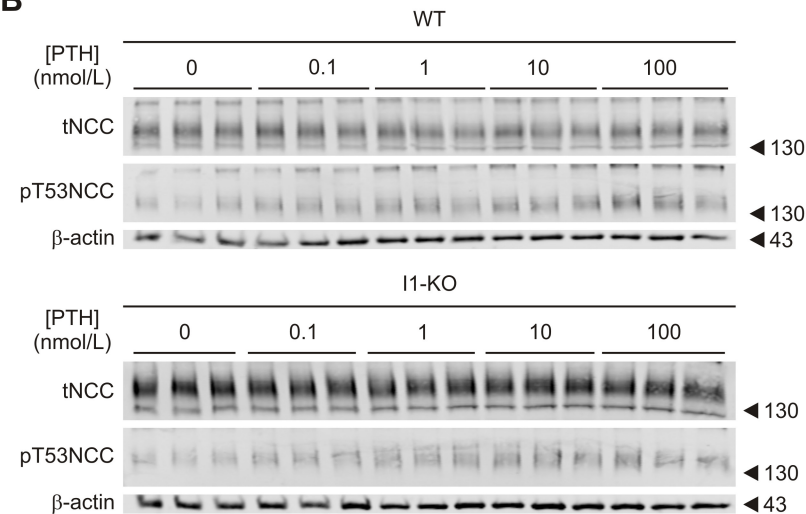
Figure 6: β -adrenergic stimulation promotes the phosphorylation of I1 at threonine 35 in native DCTs. **A:** Representative immunofluorescence stainings of tI1, pT35I1, tNCC and pT53NCC in consecutive sections of kidney slices from WT mice are shown. Slices were treated with isoproterenol 100 nmol/L or vehicle (scale bar 25 μ m). **B:** The graph represents the relative mean intensity of pT35I1 staining (left panel) or pT53NCC (middle panel) in 6-7 slices (in brackets) from 3 mice (see supplementary methods for details). Error bars represent the standard error of the mean (SEM). * $p < 0.05$, ** $p < 0.01$ assessed by unpaired Student's t-test. Right panel represents the linear correlation between I1 (pT35) and NCC (pT53) phosphorylation. **C:** Higher magnification of typical pT35I1 staining in kidney slices treated with vehicle (left panel) and isoproterenol (right panel) highlighting its marked apical accumulation. (scale bar 25 μ m)

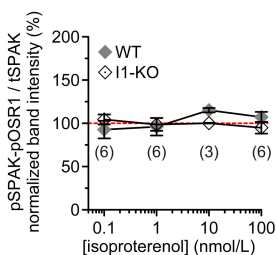
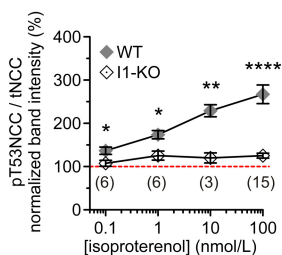
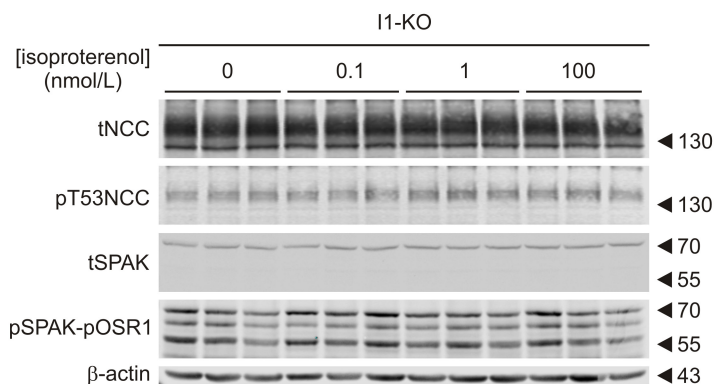
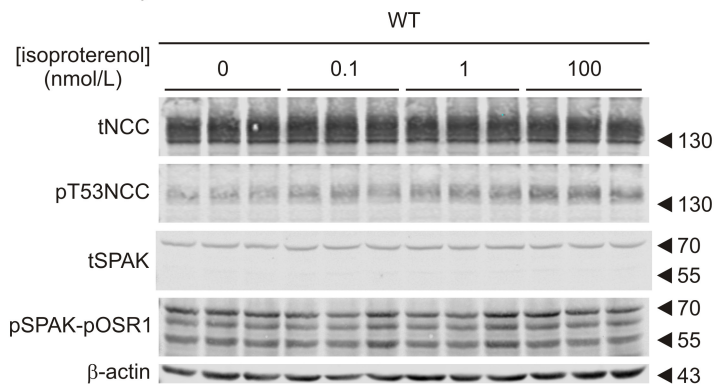
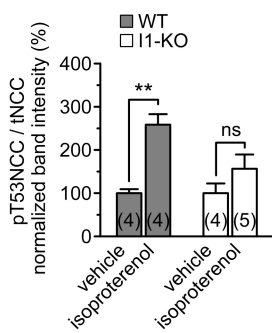
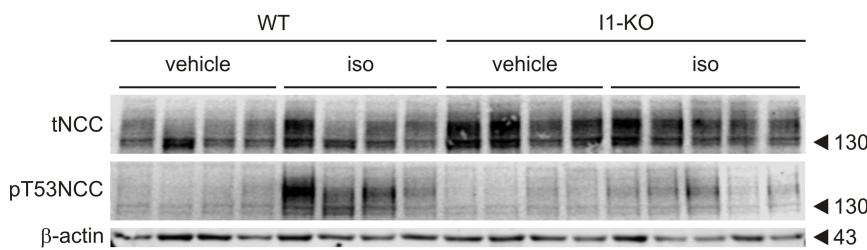
Figure 7: Model of the stimulation of NCC phosphorylation by cAMP-increasing hormones. The cAMP-dependent activation of the WNK/SPAK/OSR1 pathway was shown in previous studies^{13,15,53}. The cAMP-dependent activation of the I1/PP1 pathway is presented in the current study.

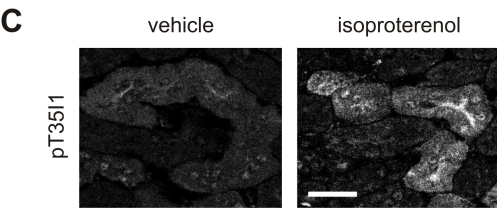
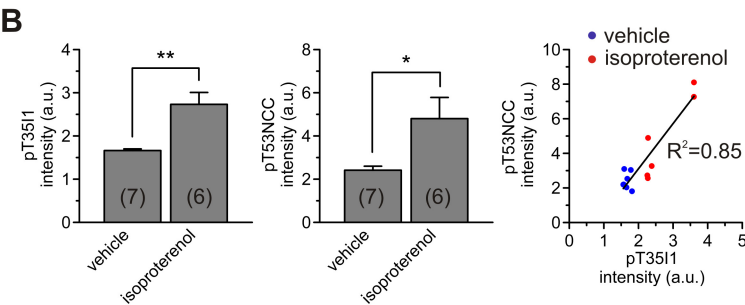
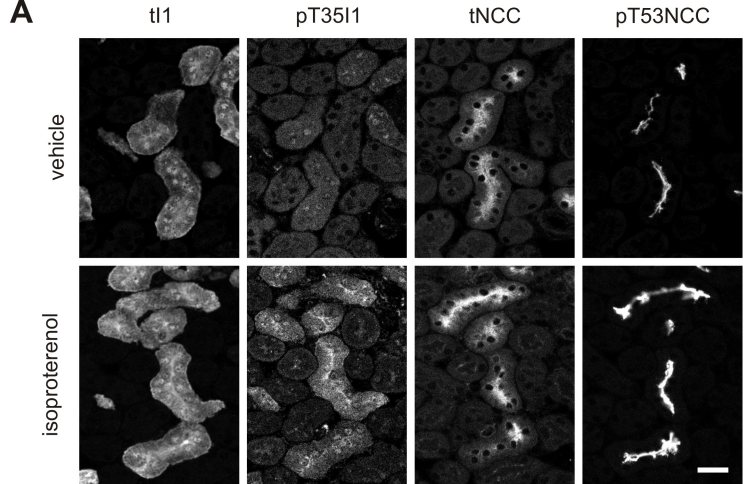


A**B****C**

A**B****C****D**

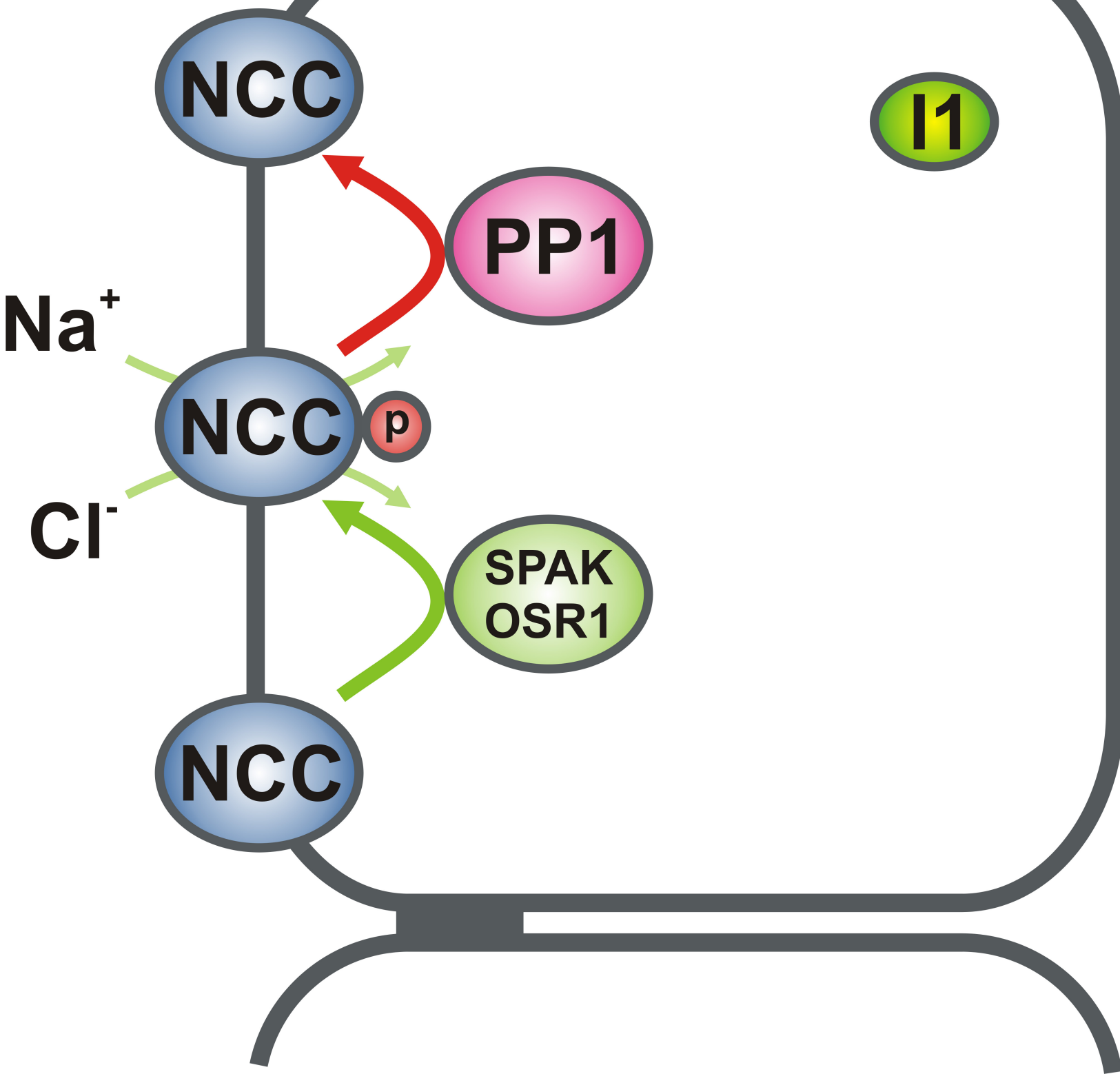
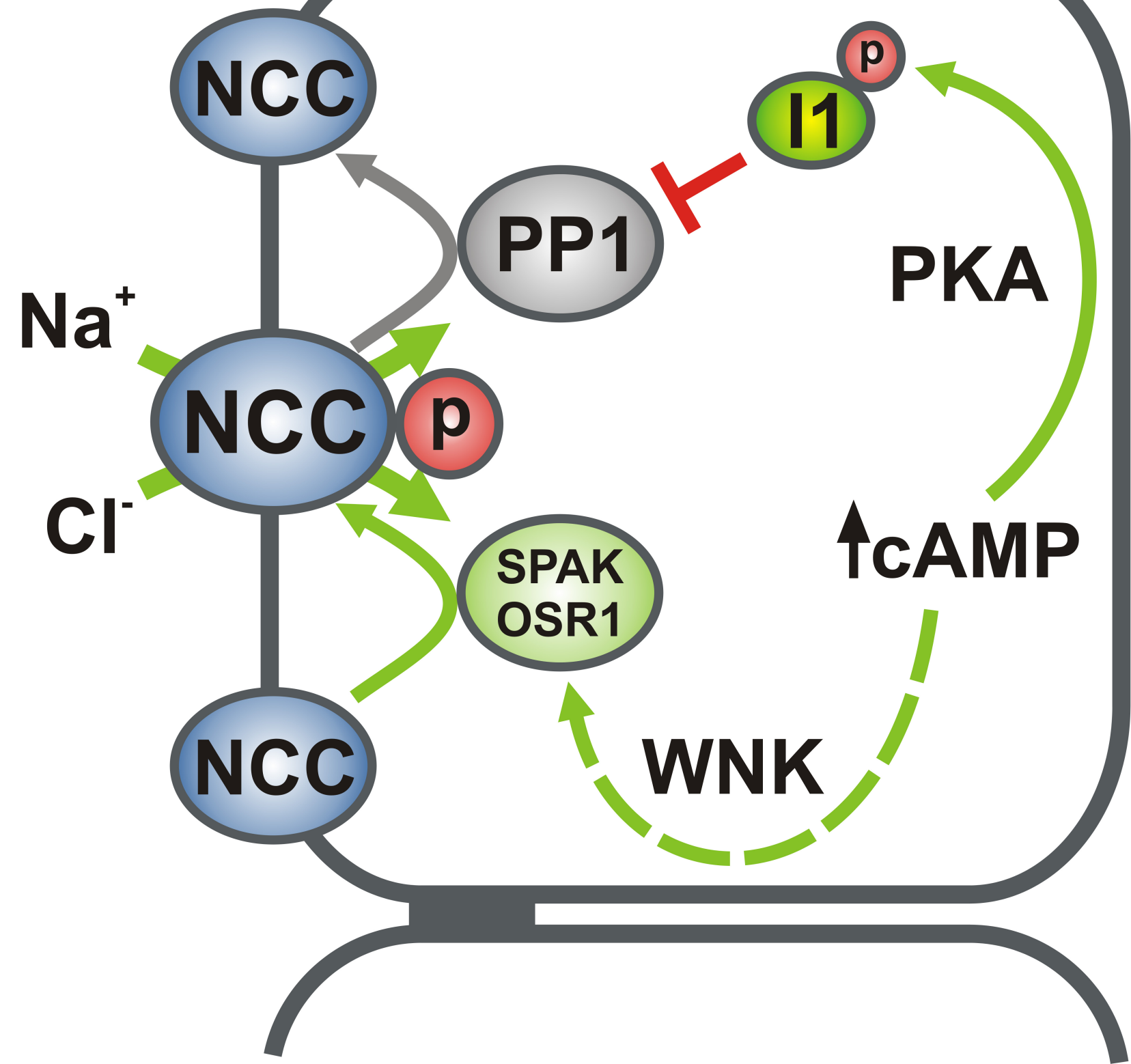
A**B**

A Mouse Kidney Slices**B** Isolated Perfused Mouse Kidney



Non Stimulated

The diagram illustrates the non-stimulated state of the I1 signaling pathway. On the left, a red oval labeled 'PP1' is shown. To its right is a green oval labeled 'I1'. Below the 'PP1' oval is a green oval labeled 'SPAK' and 'OSR1'. A red line connects the 'PP1' oval to the 'I1' oval, and a green line connects the 'SPAK' and 'OSR1' oval to the 'I1' oval. The entire diagram is enclosed in a rounded rectangle with a thick grey border.

[illegible]

I1 mediates cAMP stimulation of NCC

Supplemental material Table of content:

- Detailed methods
- Supplementary Figure 1: Assessment of the specificity of the I1-T35D antibody by immunohistochemistry
- Supplementary Figure 2: Assessment of DCT integrity in kidney slices via electron microscopy
- Supplementary Figure 3: Inhibition of cAMP-dependent phosphorylation of NCC by the PKA inhibitor H-89
- Supplementary Figure 4: Stimulation of NCC phosphorylation at T58 and S71 with cAMP elevating agents
- Supplementary Figure 5: Effect of low Cl⁻ on the stimulation of NCC and SPAK-OSR1 phosphorylation by isoproterenol in kidney slices of WT mouse
- Supplementary Figure 6: Expression of OSR1 in WT and I1-KO mice
- Supplementary table 1
- Supplementary table 2
- References

I1 mediates cAMP stimulation of NCC

Detailed methods

Yeast two hybrid

A yeast two hybrid (Y2H) screen was performed by Hybrigenics (Hybrigenics Services, S.A.S., Paris, France (<http://www.hybrigenics-services.com>)) on a mouse total kidney library with the first 133 amino acids of rat NCC as the bait fragment.

Immunoprecipitation

MDCK type I cells with tetracycline inducible FLAG-tagged NCC expression were grown until confluent on polyester supports and induced for 18 hrs with tetracycline (1 µg/µl). Cells were lysed in 20 mM Tris, 150 mM NaCl, 1% Triton-X, 0.01% SDS, pH 7.4, containing protease inhibitors Leupeptin and Pefabloc and phosphatase inhibitor mixture tablets (PhosSTOP, Roche Diagnostics). NCC was immunoprecipitated (IP) from the cleared lysate using a rabbit anti-FLAG antibody. Similar IPs without antibody or use of an AQP1 antibody served as a negative control.

Immunofluorescence staining and quantification

6-7 acute kidney slices (280 µm) from 3 mice (3 independent experiments) were prepared and incubated with isoproterenol 100 nmol/L or vehicle as described before. After stimulation, slices were fixed by immersion in 3% paraformaldehyde (PFA) prepared in 0.1 mol/L phosphate buffer (pH 7.4, 300 mOsm). After washing in similar buffer without PFA, whole slices were mounted on an organic support, frozen in liquid propane and sectioned (4 µm) to proceed with immunofluorescence staining as previously described ¹.

For the quantification of fluorescence intensity, at least two sets of 4 consecutive sections (4 µm) per slice (280 µm) were stained with the following primary antibodies tI1, pT35I1, tNCC and pT53NCC. The sections were imaged (1 image / 4 µm section) using a Leica SP8 inverse STED 3X confocal microscope equipped with a 20X multi-immersion objective (HC PL APO CS2). Within each image, all DCTs that could be identified in all four consecutive sections were selected for quantification (4-15 DCTs / image). The mean fluorescence intensity of the whole DCT was quantified using ImageJ and divided by the mean intensity of a non-stained area of the same image to correct for background differences. The intensities of all DCTs within one image were averaged to obtain one value per image per antibody. Similarly, the intensity of all

I1 mediates cAMP stimulation of NCC

images coming from the same 280 μm slice stained with the same antibody were averaged to obtain one value per slice which is represented in figure 6.

Isolated perfused mouse kidney

Isolated mouse kidney perfusion was performed at 37°C in a small animal perfusion system (Hugo Sachs Elektronik, Germany) as previously described ². To reduce the scattering of NCC activation between animals, the Renin-Angiotensin-Aldosterone System (RAAS) was suppressed 2 days prior to the experiment by feeding age and weight matched male WT and I1 deficient mice with 8% NaCl diet. In all experiments, kidneys were perfused for 40 minutes with control buffer before isoproterenol was added to a final concentration of 100 nmol/L. Kidneys were further perfused for another 40 minutes and finally snap frozen in liquid nitrogen for western blot analysis.

Electron Microscopy

Kidney slices were cut with a vibratome as described before and incubated in control buffer for 0, 30 or 60 min. Afterwards, slices were fixed overnight in 3% PFA and 1% glutaraldehyde in 0.1 mol/L phosphate buffer pH 7.3, 300 mOsm. The slices were then rinsed in 0.1 mol/L phosphate buffer before post-fixation in 1% osmium tetroxide in phosphate buffer for 2h at room temperature. Following dehydration through a graded series of ethanol, the slices were infiltrated and embedded in Epoxy embedding medium (Fluka, Seelze, Germany) overnight at room temperature. Thin sections (70 – 75 nm) were cut on a Leica EM FCS ultramicrotome and collected onto 100 mesh copper grids. Sections were stained with uranyl acetate 30 min and Reynold's lead citrate 10 min. Grids were analyzed on a Philips CM 100 (Eindhoven, The Netherlands) at 80 kV.

Automated DCT isolation

To sort single renal DCT1 fragments, mice expressing EGFP under the control of the parvalbumin promoter (PV-EGFP) ³ were anesthetized with isoflurane (Attane, Piramal, India) and perfused through the heart first with 10 ml of cold PBS and then with 10 ml of digestion solution (1mg/ml collagenase (Worthington Biochemical Corporation, Lakewood, NJ08701, USA); 1mg/ml hyaluronidase and 0.1mg/ml DNaseI prepared in ice-cold KREBS (in mmol/L): 130 NaCl, 10 HEPES, 3 KCl, 1 NaH₂PO₄, 2.5 CaCl₂, 1.8 MgSO₄, 10 glucose, pH 7.3). Renal cortex from both kidneys was dissected under a stereomicroscope. Samples were finely minced and digested in 20 ml of fresh

I1 mediates cAMP stimulation of NCC

digestion solution at 30°C for 17 minutes. The tubular digest was first filtered through 250- and 212- μ m nylon sieves. The flow-through was then filtered with a 100- μ m and a 40- μ m cell strainer (Becton Dickinson Labware, Franklin Lakes, NJ). The tubules retained by the 40- μ m cell strainer were diluted with ice-cold Krebs to a total volume of 50 ml. All sortings were performed with a large particle sorter (BioSorter) instrument (Union Biometrica, Somerville, MA). The following instrument settings were used: delay 10 mS, width 6.5 mS, PMT 350 volt, sample cup pressure 8.5 psi, pre-analysis chamber pressure 4.8-5.4 psi. The sample fluid pressure was set to maintain a sort frequency of 10-20 events/s. The mixer speed was 50%. Sorted tubules were collected directly into ice-cold KREBS and centrifuged at 800g for 4 minutes.

After sorting, a suspension of 800 DCT fragments was treated with either vehicle (DMSO) or 10 μ mol/L FSK + 100 μ mol/L IBMX, or 20 μ mol/L H-89 or 1-10 μ mol/L of PKI 14-22 amide, myristoylated or a combination of FSK/IBMX plus one of the PKA inhibitors. Treatment lasted 20 min and was performed at room temperature. After treatment, samples were shortly centrifuged, the supernatant was removed and tubuli were resuspended in Laemli buffer and further processed for immunoblot as described elsewhere⁴.

I1 mediates cAMP stimulation of NCC

Supplementary figure 1: Assessment of the specificity of the pT35I1 antibody by immunohistochemistry. **A:** Consecutive sections of kidneys from WT animals stained with pT35I1 antibody (left panel), the same antibody previously incubated with the phospho-peptide NH₂-CRRRP(pT)PATL-CONH₂ (middle panel) or pre-incubated with the dephospho-peptide NH₂-CRRRPTPATL-CONH₂ (right panel). **B:** Consecutive sections of kidneys from WT animals (upper panel of three images) or I1-KO mice (lower panel of three images) stained with NKCC2, NCC and pT35I1 antibodies.

I1 mediates cAMP stimulation of NCC

Supplementary figure 2: Assessment of DCT integrity in kidney slices from WT mice immediately after slicing (left panel) or incubated in control solution during 30 min (middle panel) and 60 min (right panel). Scale bar 10 μm .

Supplementary figure 3: Inhibition of cAMP-dependent phosphorylation of NCC by the PKA inhibitor H-89. Left panel represents a typical immunoblot of isolated DCTs treated with 1) vehicle, 2) 10 $\mu\text{mol/L}$ FSK + 100 $\mu\text{mol/L}$ IBMX, 3) 20 $\mu\text{mol/L}$ H-89 and 4) FSK+IBMX+H-89 in the same concentrations previously used. Each lane corresponds to 400 DCT fragments. On the right panel, a densitometric analysis of the pT53NCC/tNCC from 5-8 independent experiments ("n" in brackets) normalized to control vehicle group (red line) is represented. * $p < 0.05$ compared to control vehicle condition and assessed by one-way ANOVA followed by Tukey's multiple comparisons test.

I1 mediates cAMP stimulation of NCC

Supplementary figure 4: Stimulation of NCC phosphorylation at T58 and S71 with cAMP elevating agents. Representative immunoblots showing the effect of (A) IBMX (100 $\mu\text{mol/L}$), (B) forskolin (10 $\mu\text{mol/L}$) and (C) 8-Br-cAMP (10 $\mu\text{mol/L}$) on NCC phosphorylation at position T58 and S71 in WT and I1-KO kidney slices. The densitometric quantification of the immunoblots is available in supplementary table 1.

I1 mediates cAMP stimulation of NCC

Supplementary figure 5: Effect of low Cl^- on the stimulation of NCC and SPAK-OSR1 phosphorylation by isoproterenol in kidney slices of WT mouse. Graph represents the densitometric analysis of the phosphorylation of NCC at T53 (left) or the 70 KDa band of pSPAK-pOSR1 immunoblot (right) normalized to control vehicle. * $p < 0.05$, ** $p < 0.01$, ns: non-significant assessed by one-way ANOVA followed by Tukey's multiple comparisons test. $n = 3$ slices (in brackets) from 1 mouse.

I1 mediates cAMP stimulation of NCC

Supplementary figure 6: Expression of OSR1 in WT and I1-KO mice. The graph represents the densitometric quantification of tOSR1/ β -actin in all bands shown normalized to WT.

I1 mediates cAMP stimulation of NCC

Supplementary table 1: Densitometric quantification of Supplementary Figure 4

Summary					
FSK stimulation					
	mean	SEM	n	Two-way-ANOVA + Tukey's multiple comparisson	adjusted p value
WT_vehicle_pT58NCC	1	0.094367	3	WT vehicle vs FSK	<0.0001
WT_FSK_pT58NCC	2.499423	0.081614	3	I1-Ko vehicle vs FSK	0.0029
I-1_KO_vehicle_pT58NCC	1	0.070559	3	WT FSK vs I1-KO FSK	0.0051
I-1_KO_FSK_pT58NCC	1.784053	0.147475	3		
WT_vehicle_pS71NCC	1	0.073505	3	WT vehicle vs FSK	<0.0001
WT_FSK_pS71NCC	2.691473	0.169197	3	I1-KO vehicle vs FSK	0.006
I-1_KO_vehicle_pS71NCC	1	0.072473	3	WT FSK vs I1-KO FSK	0.0039
I-1_KO_FSK_pS71NCC	1.815317	0.136574	3		
IBMX stimulation					
	mean	SEM	n	Two-way-ANOVA + Tukey's multiple comparisson	adjusted p value
WT_vehicle_pT58NCC	1	0.083918	3	WT vehicle vs IBMX	<0.0001
WT_IBMX_pT58NCC	2.290356	0.080265	3	I1-KO vehicle vs IBMX	0.1023
I-1_KO_vehicle_pT58NCC	1	0.047617	3	WT IBMX vs I1-KO IBMX	<0.0001
I-1_KO_IBMX_pT58NCC	1.300646	0.095564	3		
WT_vehicle_pS71NCC	1	0.159223	3	WT vehicle vs IBMX	0.0039
WT_IBMX_pS71NCC	1.936363	0.184994	3	I1-KO vehicle vs IBMX	0.1004
I-1_KO_vehicle_pS71NCC	1	0.068808	3	WT IBMX vs I1-KO IBMX	0.1493
I-1_KO_IBMX_pS71NCC	1.494105	0.047443	3		
8-Br-cAMP stimulation					
	mean	SEM	n	Two-way-ANOVA + Tukey's multiple comparisson	adjusted p value
WT_vehicle_pT58NCC	0.991639	0.107951	3	WT vehicle vs 8-Br-cAMP	0.0008
WT_8-Br-cAMP_pT58NCC	1.970833	0.118414	3	I1-KO vehicle vs 8-Br-cAMP	0.9156
I-1_KO_vehicle_pT58NCC	1.051336	0.034929	3	WT 8-Br-cAMP vs I1-KO 8-Br-cAMP	0.0025
I-1_KO_8-Br-cAMP_pT58NCC	1.146948	0.132396	3		
WT_vehicle_pS71NCC	1.272917	0.166387	3	WT vehicle vs 8-Br-cAMP	0.0008
WT_8-Br-cAMP_pS71NCC	2.193591	0.214361	3	I1-KO vehicle vs 8-Br-cAMP	0.9156
I-1_KO_vehicle_pS71NCC	1.506866	0.130078	3	WT 8-Br-cAMP vs I1-KO 8-Br-cAMP	0.0025
I-1_KO_8-Br-cAMP_pS71NCC	1.769712	0.217122	3		

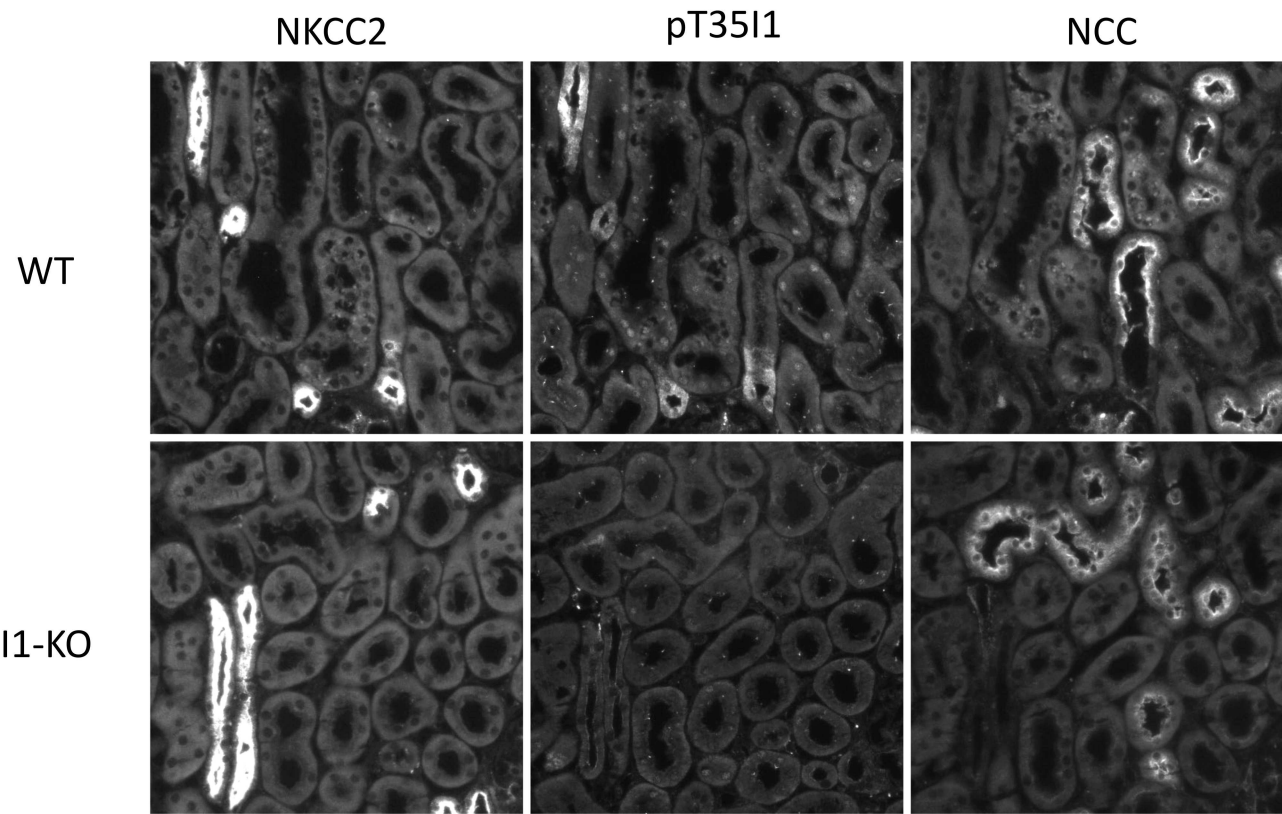
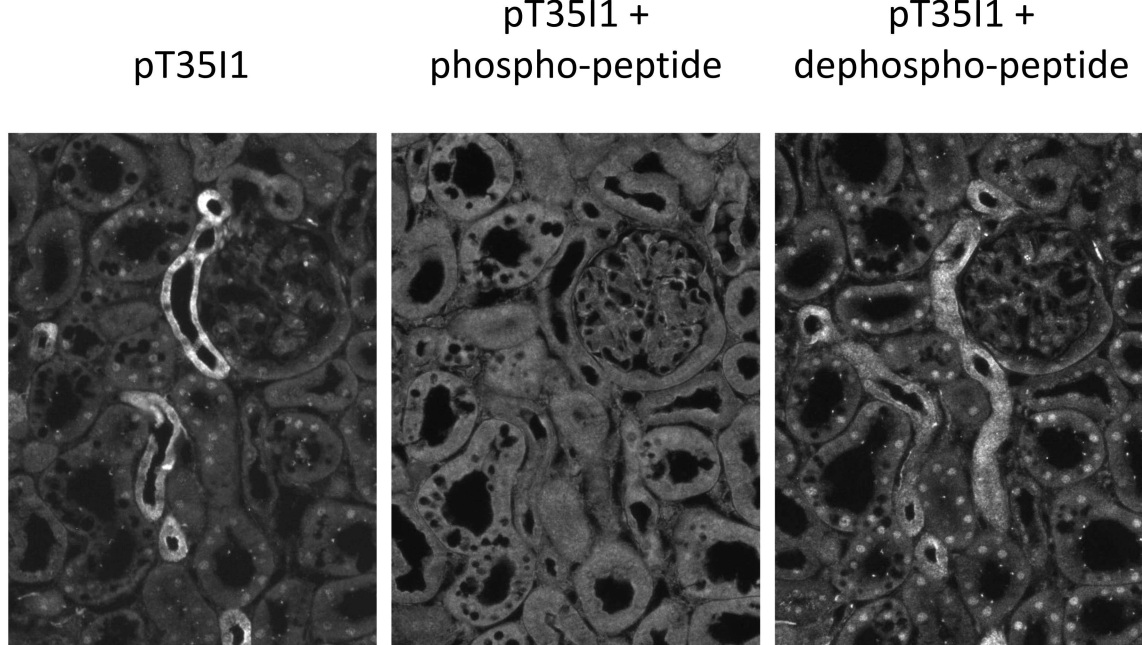
I1 mediates cAMP stimulation of NCC

Supplementary table 2: Densitometric quantification of pT58NCC shown in figure 3D of the main manuscript

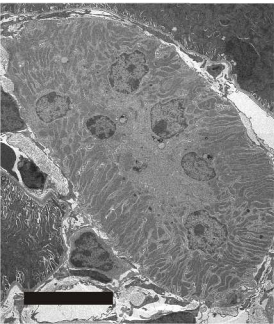
	mean	SEM	n
pT58NCC wt vehicle	1.00	0.09	3
pT58NCC WT Calyc_A	2.01	0.20	3
pT58NCC I1-KO vehicle	1.00	0.13	3
pT58NCC I1-KO Calyc_A	2.18	0.42	3

References

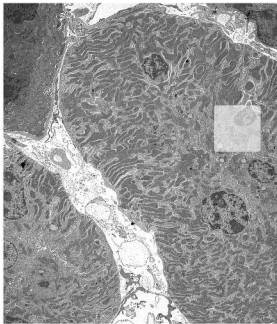
1. Picard N, Trompf K, Yang C-L, Miller RL, Carrel M, Loffing-Cueni D, Fenton RA, Ellison DH, Loffing J: Protein phosphatase 1 inhibitor-1 deficiency reduces phosphorylation of renal NaCl cotransporter and causes arterial hypotension. *J. Am. Soc. Nephrol.* 25: 511–22, 2014
2. Czogalla J, Schweda F, Loffing J: The Mouse Isolated Perfused Kidney Technique. *J. Vis. Exp.* 2016
3. Meyer AH, Katona I, Blatow M, Rozov A, Monyer H: In vivo labeling of parvalbumin-positive interneurons and analysis of electrical coupling in identified neurons. *J. Neurosci.* 22: 7055–7064, 2002
4. Penton D, Czogalla J, Wengi A, Himmerkus N, Loffing-Cueni D, Carrel M, Rajaram RD, Staub O, Bleich M, Schweda F, Loffing J: Extracellular K(+) rapidly controls NaCl cotransporter phosphorylation in the native distal convoluted tubule by Cl(-) -dependent and independent mechanisms. *J. Physiol.* 594: 6319–6331, 2016



0 min



30 min



60 min

